Bioorganic & Medicinal Chemistry xxx (xxxx) xxx–xxx

Contents lists available at ScienceDirect

Bioorganic & Medicinal Chemistry

journal homepage: www.elsevier.com/locate/bmc

Identification of novel lysine demethylase 5-selective inhibitors by inhibitor-based fragment merging strategy

Yuka Miyake[a], Yukihiro Itoh[a], Atsushi Hatanaka[b], Yoshinori Suzuma[b], Miki Suzuki[a], Hidehiko Kodama[b], Yoshinobu Arai[b], Takayoshi Suzuki[a,c,*]

[a] Graduate School of Medical Science, Kyoto Prefectural University of Medicine, 1-5 Shimogamo-hangi-cho, Sakyo-ku, Kyoto 603-0823, Japan
[b] Nippon Pharmaceutical Chemicals Co., Ltd., 2-8-18 Higashiosaka-shi, Osaka 577-0056, Japan
[c] CREST, Japan Science and Technology Agency (JST), 4-1-8 Honcho, Kawaguchi, Saitama 332-0012, Japan

ARTICLE INFO

Keywords:
JHDM
KDM
Histone methylation
Epigenetics
Inhibitor design

ABSTRACT

Histone lysine demethylases (KDMs) have drawn much attention as targets of therapeutic agents. KDM5 proteins, which are Fe(II)/α-ketoglutarate-dependent demethylases, are associated with oncogenesis and drug resistance in cancer cells, and KDM5-selective inhibitors are expected to be anticancer drugs. However, few cell-active KDM5 inhibitors have been reported and there is an obvious need to discover more. In this study, we pursued the identification of highly potent and cell-active KDM5-selective inhibitors. Based on the reported KDM5 inhibitors, we designed several compounds by strategically merging two fragments for competitive inhibition with α-ketoglutarate and for KDM5-selective inhibition. Among them, compounds **10** and **13**, which have a 3-cyano pyrazolo[1,5-*a*]pyrimidin-7-one scaffold, exhibited strong KDM5-inhibitory activity and significant KDM5 selectivity. In cellular assays using human lung cancer cell line A549, **10** and **13** increased the levels of trimethylated lysine 4 on histone H3, which is a specific substrate of KDM5s, and induced growth inhibition of A549 cells. These results should provide a basis for the development of cell-active KDM5 inhibitors to highlight the validity of our inhibitor-based fragment merging strategy.

1. Introduction

Histone lysine residues are enzymatically and post-translationally modified in cells, e.g., they are acylated and methylated.[1–3] These modifications control epigenetic gene expression independently of the DNA sequence, and are involved in various biological events, such as cell cycle, differentiation, and oncogenesis.[4–8] Therefore, the enzymes that modulate these modifications are attractive as targets of biological tools and therapeutic agents to chemical biologists and medicinal chemists in the field of epigenetics.[9–12]

Histone lysine demethylases (KDMs) are classified into two groups: FAD-dependent demethylases (lysine-specific demethylases, LSDs; also known as KDM1s) and Fe(II)/α-ketoglutarate-dependent demethylases (jumonji C domain-containing histone demethylases, JHDMs).[13–16] Both enzymes are attractive as therapeutic targets for various diseases. LSDs are overexpressed in several cancer cells and associated with oncogenesis.[17–20] Indeed, some LSD1 inhibitors are currently being tested in clinical trials.[21,22] JHDMs are also regarded as targets for the therapy of some diseases, such as cancer and inflammatory diseases.[23–26] However, no JHDM inhibitors are being clinically tested. Thus, drug discovery studies of JHDM inhibitors are relatively delayed.

JHDMs have different subfamilies, including KDM2–8.[27] Among the JHDM family proteins, KDM5s have been viewed as targets for cancer therapy.[28,29] The KDM5 family is composed of four members (KDM5A–D) that catalyze the demethylation of tri- and dimethylated lysine 4 on histone H3 (H3K4me3/me2).[28,29] KDM5A is a member of polycomb complexes and is deeply involved in gene repression.[30] KDM5A is overexpressed in several human cancer cells, such as lung and breast cancer cells, and is associated with cancer cell proliferation and drug resistance.[31–33] KDM5B is also overexpressed in human cancer cells, and is involved in the proliferation of cancer cells through the E2F/RB pathway.[34] KDM5C and KDM5D are overexpressed in prostate cancer cells and may play critical roles in the cell proliferation.[35–37] Based on these backgrounds, KDM5-selective inhibitors that are active in cells or animals are required for both chemical biology studies of KDM5 and new cancer therapy.

Some KDM5 inhibitors have been reported.[38–43] In 2015, we identified NCDM-81a (**1a**) and NCDM-82a (**2a**) (Fig. 1) as KDM5 inhibitors,

* Corresponding author at: Graduate School of Medical Science, Kyoto Prefectural University of Medicine, 1-5 Shimogamo-hangi-cho, Sakyo-ku, Kyoto 603-0823, Japan.
E-mail address: suzukit@koto.kpu-m.ac.jp (T. Suzuki).

https://doi.org/10.1016/j.bmc.2019.02.006
Received 25 December 2018; Received in revised form 23 January 2019; Accepted 1 February 2019

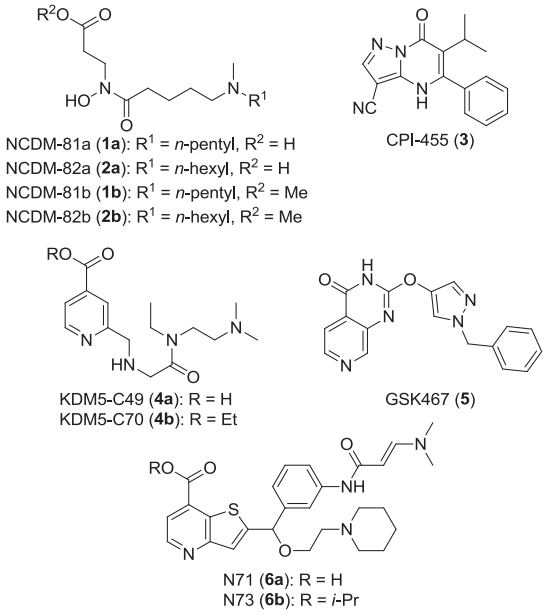

Figure 1. Structures of representative KDM5 inhibitors.

although their IC_{50} values were in the micromolar range and KDM5 selectivities were moderate.[44] In 2016, three potent and selective KDM5 inhibitors, CPI-455 (**3**), KDM5-C49 (**4a**), and GSK467 (**5**), were reported (Fig. 1).[45,46] Furthermore, in 2018, N71 (**6a**) was identified as a covalent KDM5 inhibitor.[47] However, their cellular activities were extremely weak and a high concentration was needed for cellular study even if their prodrug forms, namely, NCDM-81b (**1b**), NCDM-82b (**2b**), KDM5-C70 (**4b**), and N73 (**6b**) (Fig. 1), were used. These KDM5-selective inhibitors warrant improvements. In this study, we attempted to identify novel KDM5-selective inhibitors that are active in cells at low concentrations. To this end, we designed compounds by strategic fragment merging of two fragments for competitive inhibition with α-ketoglutarate and for KDM5-selective inhibition, focusing on the structures of the reported KDM5 inhibitors. Through this, we identified highly potent and selective KDM5 inhibitors **10** and **13**. We also found that **10** and **13** induced the trimethylation of H3K4 in cells and more strongly inhibited the growth of cancer cells than CPI-455 (**3**). Herein, we present our drug discovery study of KDM5-selective inhibitors.

2. Chemistry

The compounds tested in this study are described in Fig. 3 and Table 2. The compounds were prepared by the synthetic routes shown in Schemes 1–4. Scheme 1 shows the preparation of compound **7**. Phthalimide was reacted with 1,2-dibromoethane and subsequently with *N*-hexylmethylamine to obtain compound **14**. Phthalimide **14** was converted into diamine **15** in the presence of hydrazine. Oxidation of 4,4′-dimethyl-2,2′-bipyridine in the presence of potassium permanganate and esterification under the acidic condition gave diester **17**. Monohydrolysis of **17** under the basic condition yielded **18**. Condensation of **15** and **18** afforded **19**. Compound **19** was treated with NaOH solution to give **7**.

Compound **8** was prepared from *N*-(3-bromopropyl)phthalimide and 2,4-pyridinedicarboxylic acid by using a similar route to the one used for the preparation of **7** (Scheme 2). Compound **21** was synthesized by an S_N2 reaction of *N*-(3-bromopropyl)phthalimide with *N*-hexylmethylamine, and this was followed by the removal of the phthalimide scaffold. Compound **23** was obtained by the diesterification of 2,4-pyridinedicarboxylic acid and the subsequent monohydrolysis of diester **22**. Condensation of **21** and **23** yielded **24**. Hydrolysis of **24** under the basic condition gave **8**.

Compound **9** was prepared from quinoxaline-2,3(1*H*,4*H*)-dione by the procedure outlined in Scheme 3. The reaction of quinoxaline-2,3(1*H*,4*H*)-dione with ethyl bromoacetate followed by treatment with bromo-3-chloropropane in the presence of sodium hydride in DMF gave compound **26**. Then, **26** was allowed to react with *N*-hexylmethylamine to give compound **27**. Finally, the ethyl ester of **27** was converted into carboxylic acid to obtain compound **9**.

Compounds **10–13** were synthesized as outlined in Scheme 4. 5-Amino-1*H*-pyrazole-4-carbonitrile was reacted with diethyl 2-isopropylmalonate to obtain compound **28**. Dichlorination of compound **28** and a subsequent reaction with sodium hydroxide furnished compound **29**. Oxidation of 2-(4-bromophenyl)ethanol by Dess-Martin periodinane gave aldehyde **30**. Compounds **31** were prepared from aldehyde **30** or 4-bromothiophene-2-carbaldehyde by reductive amination. Pinnacol borates **32** were prepared by S_N2 reactions of benzyl bromides with *N*-hexylmethylamine (for compounds **32a** and **32b**) or coupling reactions in the presence of palladium catalyst of bis(pinacolate)diboron with bromides **31** (for compounds **32c** and **32d**). Suzuki coupling of compound **29** with pinacol borates **32** provided desired compounds **10–13**.

3. Results and discussion

3.1. Inhibitor design

Thus far, we have identified several KDM inhibitors consisting of a hydroxamate, a carboxylate, and an alkyl chain group.[44,48,49] The hydroxamate group and the carboxylate group are essential for the competitive inhibition with α-ketoglutarate, which is a co-enzyme of JHDMs: the hydroxamate works as a Fe(II) chelator in the KDM catalytic site, and the carboxylate corresponds to the carboxylate group of α-ketoglutarate (Fig. 2A). However, these two groups decrease the

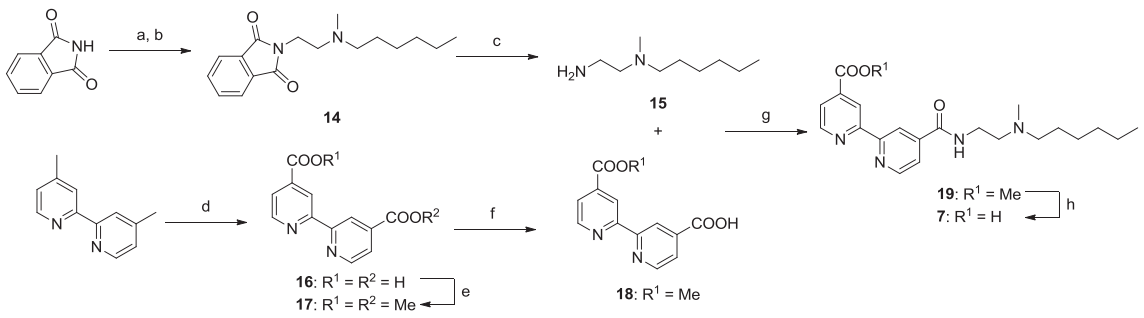

Scheme 1. Reagents and reaction conditions: (a) 1,2-dibromoethane, K_2CO_3, DMF, room temperature, 2 h, 34%; (b) *N*-hexylmethylamine, K_2CO_3, DMF, 100 °C, 3 h, 46%; (c) $N_2H_4{\cdot}H_2O$, EtOH, reflux, 2 h, 91%; (d) $KMnO_4$, H_2O, reflux, 6 h, 99%; (e) $SOCl_2$, MeOH, reflux, overnight, 91%; (f) NaOH, THF, MeOH, H_2O, room temperature, overnight, 84%; (g) EDCI·HCl, HOBt, Et_3N, DMF, room temperature, overnight, 12% (from **18**); (h) NaOH, THF, MeOH, H_2O, room temperature, overnight, 60%.

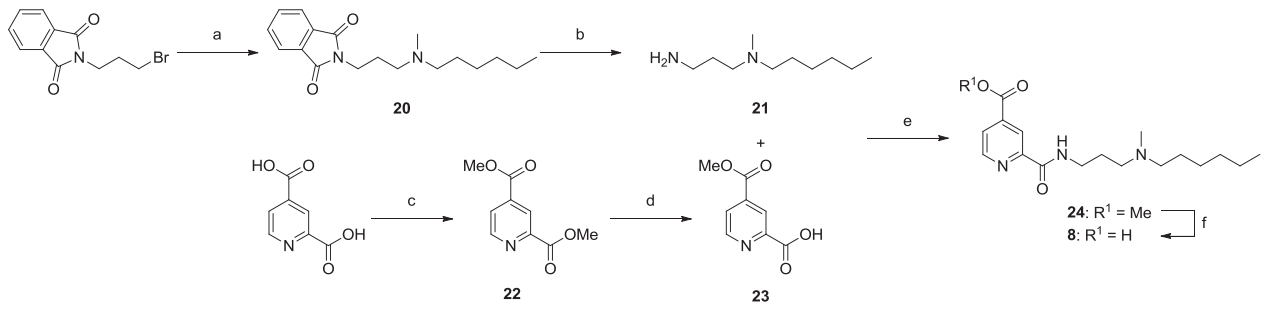

Scheme 2. Reagents and reaction conditions: (a) *N*-hexylmethylamine, K_2CO_3, MeCN, reflux, 1 h, 84%; (b) $N_2H_4{\cdot}H_2O$, EtOH, reflux, 2.5 h, 75%; (c) $SOCl_2$, MeOH, reflux, 5 h, 89%; (d) KOH, MeOH, reflux, 1 h; (e) EDCI·HCl, HOBt, Et_3N, DMF, 70 °C, 4.5 h, 32% (from **21**); (f) KOH, MeOH, reflux, 1 h, 87%.

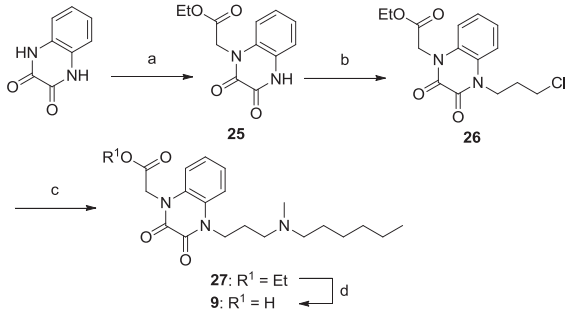

Scheme 3. Reagents and reaction conditions: (a) Ethyl bromoacetate, NaH, DMF, room temperature, 2 h, 25%; (b) 1-bromo-3-chlroropropane, NaH, DMF, room temperature, 2 h, 54%; (c) *N*-hexylmethylamine, K_2CO_3, MeCN, reflux, 5 h, 82%; (d) NaOH, THF, MeOH, H_2O, room temperature, 2 h, 75%.

cellular activity of the KDM inhibitors because they are highly polar functional groups that result in the low membrane permeability of the KDM5 inhibitors. On the other hand, the alkyl chain is a key structure for KDM subfamily selectivity. In the case of KDM5-selective inhibitors, such as NCDM-81a (**1a**) and NCDM-82a (**2a**), an amino alkyl chain with a methyl group and a long alkyl group (*n*-pentyl or *n*-hexyl group) is preferred (Fig. 2A).[44] Furthermore, the linker length between the Fe(II) chelator part and the nitrogen atom is important for KDM5 selectivity (Fig. 2A).[44] Based on these backgrounds, we hypothesized that cell-active KDM5 inhibitors would be obtained by merging *N*-hexyl-*N*-methyl amino chain with a scaffold that is expected to compete with α-ketoglutarate and not to give rise to high polarity and low membrane permeability. As shown in Fig. 2B, we planned to use bipyridine, picolinamide, and quinoxalinedione moieties for the Fe(II) chelator part as the scaffold, and to conjugate them with carboxylate. We also attempted to use 3-cyano pyrazolo[1,5-*a*]pyrimidin-7-one, which works as a monodentate Fe(II) chelator and a carboxylate mimic (Fig. 2B). The reason why we focused on these structures was that these have been already used in KDM5 inhibitors or Fe(II) chelators; bipyridine has been used in several KDM inhibitors;[50] picolinamide and quinoxalinedione can function as a bidentate metal ion chelator[51,52] the 3-cyano pyrazolo [1,5-*a*]pyrimidin-7-one scaffold has been used in KDM5 inhibitors, such as CPI-455 (**3**).[45] The linker structures were designed based on the superposition of NCDM-82a (**2a**) on each α-ketoglutarate mimic (Fig. 3). The conformation of NCDM-82a (**2a**) docked to KDM5A, which was previously reported by our group,[44] was superimposed on the bipyridine, picolinamide and quinoxalinedione, and 3-cyano pyrazolo [1,5-*a*]pyrimidin-7-one moieties as their α-ketoglutarate mimic parts were located on the same place. Based on these superimposed structures, the linkers were designed so that the nitrogen atom of the *N*-hexyl-*N*-methyl amino chain is positioned as close to that of NCDM-82a (**2a**) as possible; a two-methylene linker for compound **7**; a three-methylene linker for compounds **8** and **9**; and a one-methylene linker for compound **10**. Thus, we designed compounds **7**–**10** by an inhibitor-based fragment merging strategy.

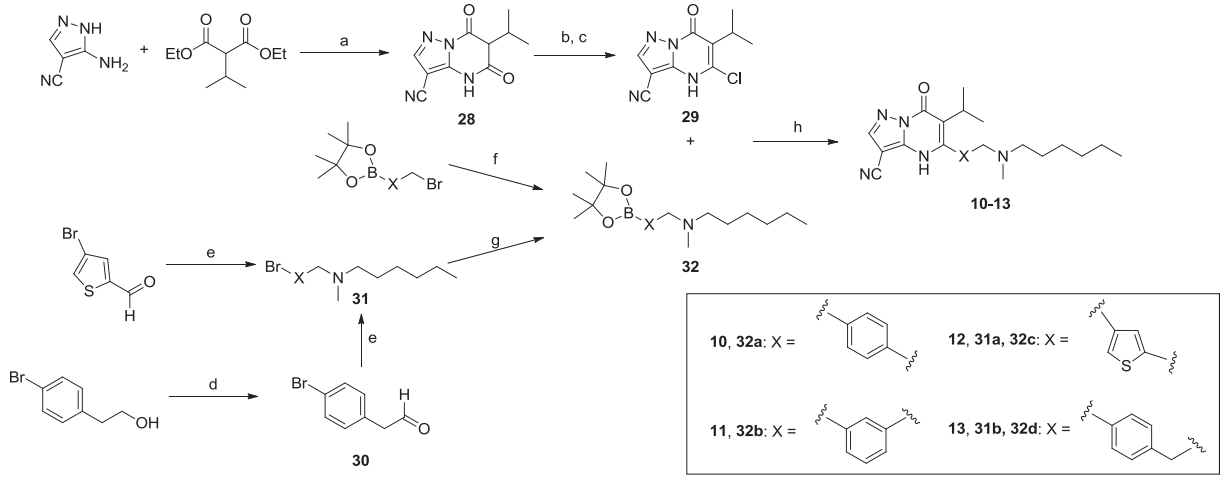

Scheme 4. Reagents and reaction conditions: (a) NaOEt, EtOH, MW 160 °C, 0.5 h, quant.; (b) $POCl_3$, MW 170 °C, 2 h, 26%; (c) NaOH, THF, H_2O, reflux, 0.75 h, 72%; (d) Dess-Martin periodinane, CH_2Cl_2, room temperature, 1 h, 62%; (e) *N*-hexylmethylamine, $NaBH(OAc)_3$, 1,2-DCE, room temperature, 5 h, 53% for **31a** or 79% for **31b**; (f) *N*-hexylmethylamine, K_2CO_3, MeCN, reflux for **32a** or room temperature for **32b**, 1 h for **32a** or overnight for **32b**, 69% for **32a** or 82% for **32b**; (g) bis (pinacolate)diboron, $PdCl_2(dppf){\cdot}CH_2Cl_2$, AcOK, dioxane, MW 140 °C, 0.5 h, 26% for **32c** or 85% for **32d**; (h) $PdCl_2(dppf){\cdot}CH_2Cl_2$, Na_2CO_3, DME, H_2O, MW 160 °C, 0.5 h, 20% for **10**, 7% for **11**, 20% for **12**, or 18% for **13**.

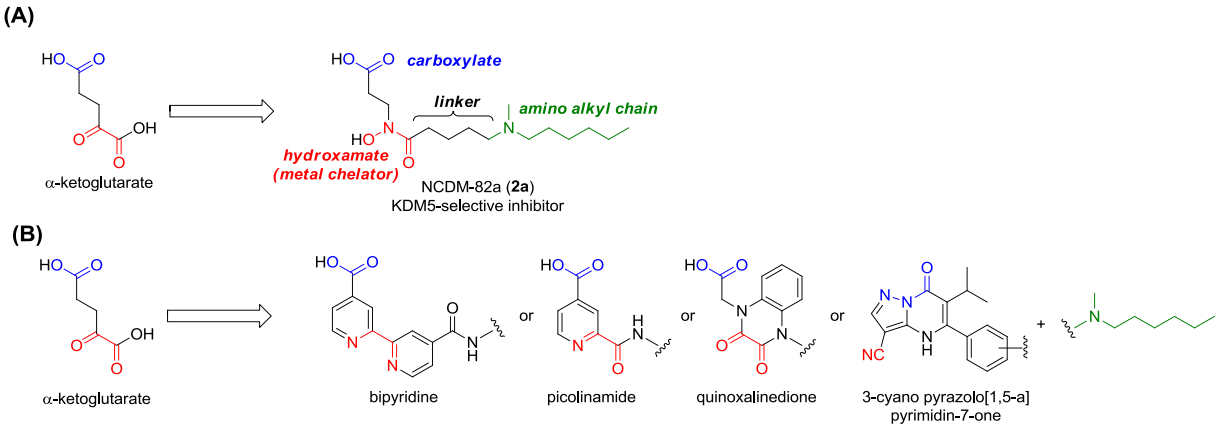

Figure 2. (A) Our previous work. (B) This work.

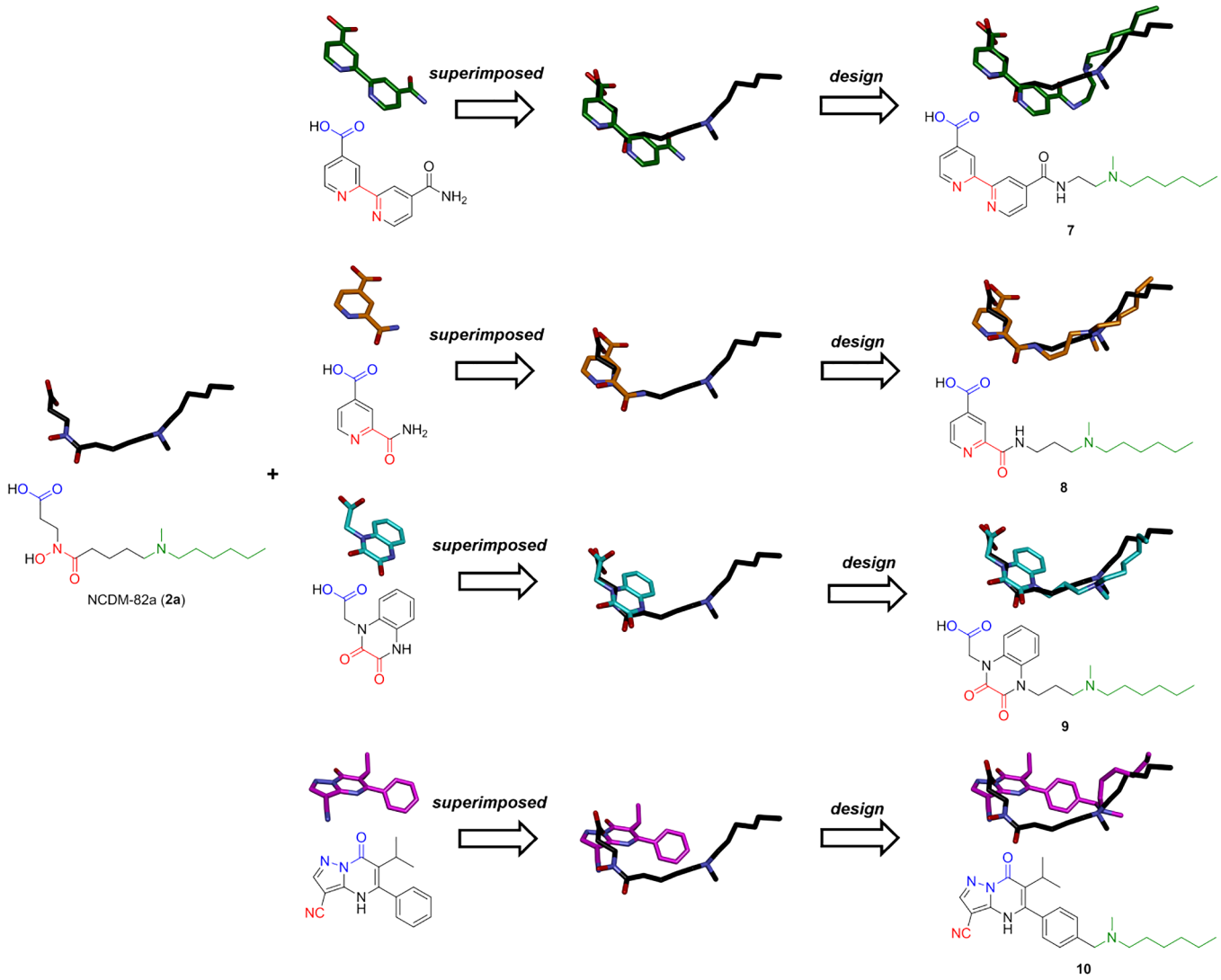

Figure 3. Drug design based on fragment merging of α-ketoglutarate mimic scaffolds and *N*-hexyl-*N*-methyl amino group.

3.2. Enzyme assay

Initially, we evaluated the KDM5A inhibitory activities of synthetic compounds **7**–**10** by conducting an AlphaLISA screen assay. We used NCDM-81a (**1a**) and CPI-455 (**3**) as positive controls, and tested the compounds at 1 or 25 μM. As shown in Table 1, bipyridine **7** inhibited KDM5A strongly, and its inhibitory activity was comparable or slightly superior to that of CPI-455 (**3**) (Table 1, entries 2 and 3). On the other hand, the inhibitory activities of picolinamide **8** and quinoxalinedione **9** were inferior to that of NCDM-81a (**1a**) (Table 1, entries 1, 4, and 5). Interestingly, 3-cyano pyrazolo[1,5-*a*]pyrimidin-7-one **10** exhibited the most potent inhibitory activity among the tested compounds.

Table 1
In vitro KDM5A inhibitory activities of NCDM-81 (**1a**), CPI-455 (**3**), and compounds **7–10**.

Entry	Compound	% Inhibition [a]	
		at 1 μM	at 25 μM
1	**1a**	30.8 ± 2.1	89.9 ± 0.9
2	**3**	68.9 ± 3.3	100 ± 0.43
3	**7**	87.0 ± 10.7	96.1 ± 3.0
4	**8**	N.D. [b]	12.0 ± 1.4
5	**9**	N.D. [b]	16.5 ± 9.9
6	**10**	97.9 ± 0.5	N.D. [b]

[a] Values represent means ± standard deviation of at least three experiments. [b] No data.

Table 2
In vitro KDM5A inhibitory activities of compounds NCDM-81 (**1a**), CPI-455 (**3**), **7**, and compounds **10–13**.[a]

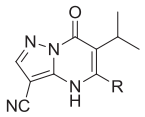

Entry	Compound	R	IC_{50} (nM)
1	**1a**	–	2700 ± 210
2	**3**	Ph	506 ± 38
3	**7**	–	170 ± 12
4	**10**	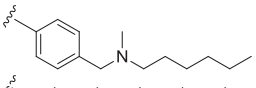	22.7 ± 3.2
5	**11**	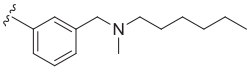	65.3 ± 8.6
6	**12**	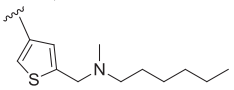	179 ± 12
7	**13**	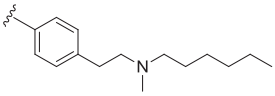	4.37 ± 0.19

[a] Values represent means ± standard deviation of at least three experiments.

Compound **10** at 1 μM almost completely inhibited KDM5A (Table 1, entry 6). Given the results, we determined the IC_{50} values of **7** and **10** for KDM5A inhibition (Table 2). The IC_{50} values of **7** and **10** were lower than those of reference compounds NCDM-81a (**1a**) and CPI-455 (**3**) (Table 2, entries 1 and 2). Especially, **10** had 22 times stronger KDM5A inhibitory activity than CPI-455 (**3**).

Subsequently, we performed the structure optimization of the linker part of **10** (Table 2). We changed the alkyl amino chain in **10** from para-position to meta-position. The KDM5A inhibitory activity of meta-substituted compound **11** was three times lower than that of **10** (Table 2, entries 4 and 5), although it was high compared to the KDM5A inhibitory activity of **7**. We also replaced the para-substituted benzene ring in **10** with a 2,4-substituted thiophene ring to yield **12**. However, the KDM5A inhibitory activity of **12** was 8 times lower than that of **10** (IC_{50} of **12**: 179 ± 12 nM), and was nearly the same as that of **7** (Table 2, entries 3 and 6). Next, we extended the methylene linker between the benzene ring and the nitrogen atom conjugating the methyl and *n*-hexyl groups. Compound **13** with a two-methylene linker exhibited potent KDM5A inhibitory activity: its activity was 5 times and 116 times greater than that of **10** and CPI-455 (**3**), respectively (Table 2, entries 2, 4, and 7). Thus, compound **13** was the strongest KDM5A inhibitor among the tested compounds.

Then, to investigate the selectivity of **10** and **13** for KDM5 enzymes, we evaluated the inhibitory activities of compounds **10**, **13**, NCDM-81a (**1a**), and CPI-455 (**3**) against KDM5B and KDM5C by AlphaLISA screen assay. The IC_{50} values of NCDM-81a (**1a**) for KDM5B and KDM5C were 9240 ± 704 nM and 28900 ± 1720 nM, respectively, which indicate that NCDM-81a (**1a**) is a relatively KDM5A-selective inhibitor (Table 3, entry 1). CPI-455 (**3**) inhibited KDM5A and KDM5B strongly compared to KDM5C (Table 3, entry 2). On the other hand, **10** showed low KDM5C selectivity (Table 3, entry 3, KDM5A IC_{50} = 22.7 ± 3.2 nM; KDM5B IC_{50} = 51.1 ± 5.3 nM; KDM5C IC_{50} = 5.84 ± 0.65 nM). Furthermore, **13** exhibited potent inhibitory activity against all the three enzymes with IC_{50} values of 1.34–6.24 nM (Table 3, entry 4, KDM5A IC_{50} = 4.37 ± 0.19 nM; KDM5B IC_{50} = 1.34 ± 0.16 nM; KDM5C IC_{50} = 6.24 ± 0.70 nM). The results of the KDM5 inhibition profiling of **10** and **13** suggest that the slight difference in the amino alkyl chain is responsible for the selectivity differences for KDM5s: optimization of the chain structure may lead us to the identity of KDM5-isozyme-selective inhibitors, although we need further studies of the structure-activity or selectivity relationships.

Finally, we confirmed the selectivity of **10** and **13** for other KDM family proteins (KDM2A, KDM3A, KDM4A, KDM6B, and KDM7B). As shown in entries 3 and 4 of Table 3, the inhibitory activities of **10** and **13** at 25 μM and 50 μM against the five enzymes were not high; we estimated that the IC_{50} values of **10** for KDM4A and **13** for KDM3A should be between 25 and 50 μM, and that the other IC_{50} values were higher than 50 μM. Thus, **10** and **13** have significantly higher KDM5 inhibitory activities than the other KDM subfamily proteins, and we conclude that they are highly potent KDM5-selective inhibitors.

3.3. Molecular docking

We performed docking simulation to understand the structural basis of KDM5A inhibition by most potent KDM5 inhibitor **13**. Compound **13** was docked to the three-dimensional structure of KDM5A (PDB ID: 5CEH) using Molegro Virtual Docker 6.0 software. As shown in Fig. 4, **13** was docked to the KDM5A active site. As is the case with CPI-455 (**3**)

Table 3
In vitro KDM inhibitory activities of NCDM-81 (**1a**), CPI-455 (**3**), **7**, and compounds **10** and **13**.[a]

Entry	Compound	IC_{50} (nM)			% inhibition at 50 μM (upper) and at 25 μM (bottom)				
		KDM5A	KDM5B	KDM5C	KDM2A	KDM3A	KDM4A	KDM6B	KDM7B
1	**1a**	2700 ± 210	9240 ± 704	28900 ± 1720	51.7 ± 3.4 N.D.	30.1 ± 4.9 N.D.	25.4 ± 3.0 N.D.	17.8 ± 2.3 N.D.	N.D. N.D.
2	**3**	506 ± 38	337 ± 144	3010 ± 1235	25.7 ± 2.2 N.D.	31.9 ± 3.1 N.D.	61.1 ± 2.5 35.9 ± 5.2	N.D. 69.1 ± 2.8[b]	N.D. N.D.
3	**10**	22.7 ± 3.2	51.1 ± 5.3	5.84 ± 0.65	13.4 ± 5.7 N.D.	61.5 ± 4.8 13.0 ± 1.4	32.5 ± 3.5 N.D.	29.1 ± 0.4 N.D.	N.D. 12.1 ± 2.9
4	**13**	4.37 ± 0.19	1.34 ± 0.16	6.24 ± 0.70	38.4 ± 6.9 N.D.	15.9 ± 5.9 N.D.	71.0 ± 3.1 32.4 ± 3.1	22.7 ± 3.1 N.D.	N.D. 11.8 ± 5.5

[a] Values represent means ± standard deviation of at least three experiments. [b] IC_{50} = 14300 ± 2250 nM.

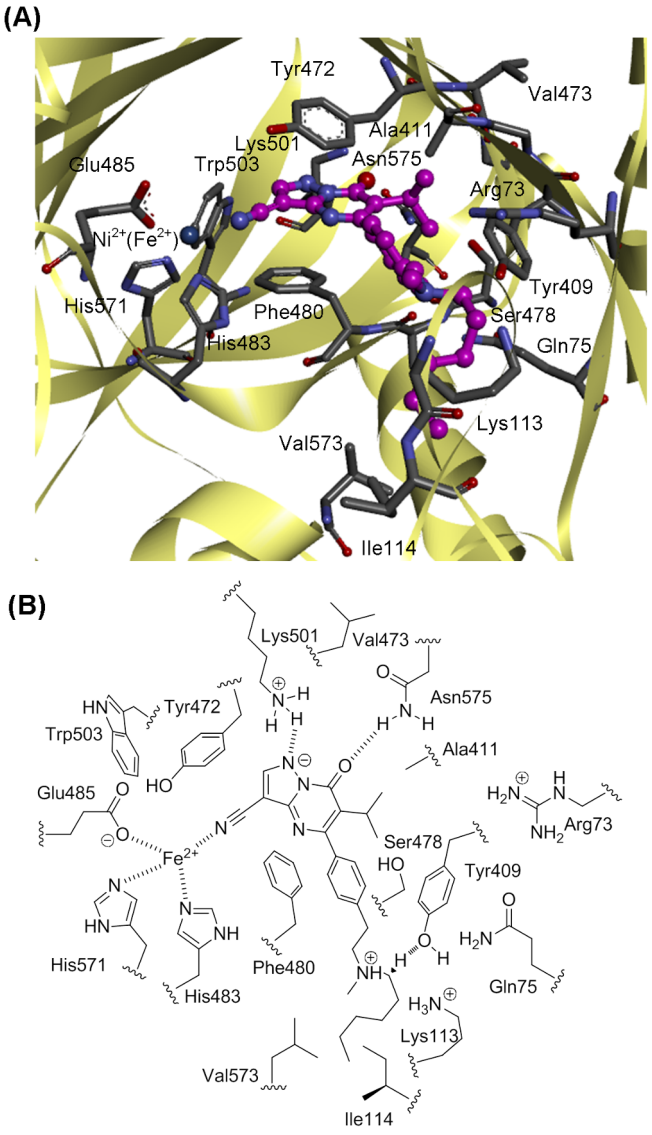

Figure 4. Docking simulation of **13** to KDM5A (PDB ID: 5CEH). (A) View of the conformation of **13** (ball-and-stick, purple carbons) docked into the KDM5A active site. (B) Schematic diagram of binding of **13** docked into the KDM5A active site. (For interpretation of the references to colour in this figure legend, the reader is referred to the web version of this article.)

(Supplementary Figure S1), the cyano group of **13** could coordinate to the catalytic Fe(II) ion and the pyrazole carbonyl group could interact with Lys501/Asn575 through hydrogen bonds. The hexyl group of **13** was located in a hydrophobic space surrounded by Lys113, Ile114, and Val573. Interestingly, a C-H group that is conjugated with the amino group was located in a position where it could form a N^+-C-H···O hydrogen bond[53] with the hydroxyl group of Tyr409. We assume that this kind of hydrogen bond is not formed between compound **10** and the hydroxyl group of Tyr409 because the methylene spacer of compound **10** is shorter than that of compound **13**. This simulation suggests that the hydrophobic interaction and the N^+-C-H···O hydrogen bond formation are important for the KDM5 inhibitory activity of **13**.

3.4. Cellular assay

Compounds **10** and **13**, which are potent KDM5-selective inhibitors, were tested in cellular assays. As KDM5A is overexpressed in human lung cancer cell line A549,[31] we used A549 cells in this study. We incubated A549 cells with compounds **10** and **13**, and after 48 h, we

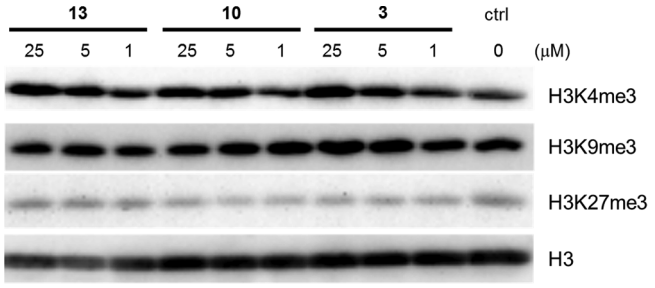

Figure 5. Western blots showing H3K4me3, H3K9me3, H3K27me3, and H3 levels in A549 cells treated with CPI-455 (**3**), **10**, and **13**. The methylation levels were analyzed after 48 h incubation with the inhibitors.

detected H3K4me3 levels by western blot analysis because H3K4me3 is a specific substrate of KDM5s.[28,29] As shown in Fig. 5, **10** and **13** at 1, 5, and 25 μM increased H3K4me3 levels in a dose-dependent manner like CPI-455 (**3**). These results indicate that compounds **10** and **13** inhibited KDM5s in A549 cells. In addition, we analyzed the influence of the inhibitors on H3K9me3 and H3K27me3, which are substrates of KDM4s and KDM6s, respectively.[13] Compounds **10** and **13** did not affect the methylation levels of H3K9me3 and H3K27me3 (Fig. 5). These results suggest that **10** and **13** selectively inhibit KDM5s in preference to other KDMs in A549 cells.

Finally, we tested the growth inhibitory activity of **10** and **13** against A549 cells because KDM5A is involved in the proliferation of A549 cells.[31] Treatment of A549 cells with 50 μM each of compounds **10** and **13** inhibited the growth of A549 cells, whereas CPI-455 (**3**) at the same concentration did not inhibit it strongly (Fig. 6A). Furthermore, we determined the half-maximal growth inhibition concentration (GI_{50}) values of **10** and **13**. As shown in Fig. 6B, **10** and **13** inhibited cell growth in a dose-dependent manner, and the GI_{50} values were 40.0 μM for **10** and 29.6 μM for **13**. The GI_{50} value of CPI-455 (**3**) was higher

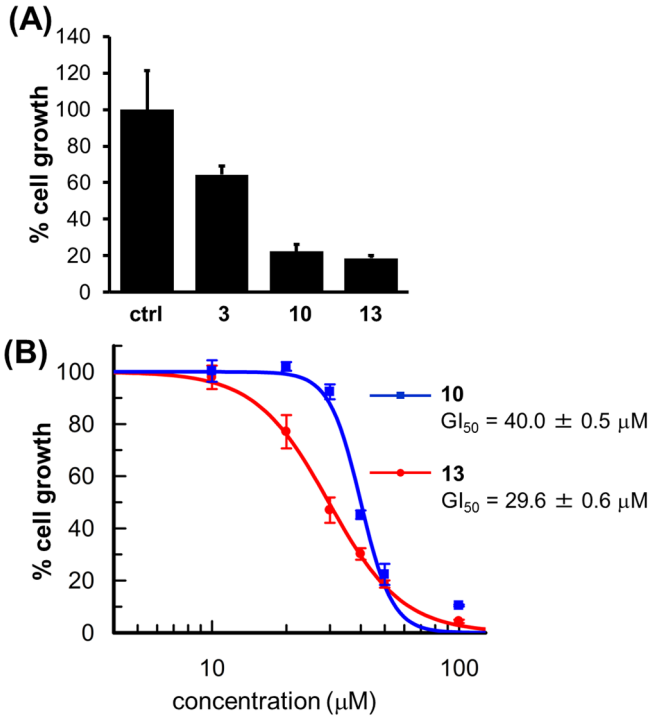

Figure 6. Growth inhibitory activity of CPI-455 (**3**), **10**, and **13** in A549 cells after treatment for 72 h. (A) Treatment of the cells with 50 μM of the inhibitors. (B) Dose-dependent curves of **10** and **13**. Values were calculated from three independent determinations. Bars represent means ± SD from three independent experiments.

than 50 μM (Fig. 6A). The GI_{50} values of CPI-455 (**3**), **10**, and **13** (GI_{50}: **3** > **10** > **13**) are consistent with their IC_{50} values in the in vitro KDM5A assay (IC_{50}: **3** > **10** > **13**) (Table 3). We also investigated the effects of CPI-455 (**3**), **10**, and **13** on breast cancer MDA-MB-231 cells where KDM5A expression level is lower than that in A549 cells (Supplementary Figure S2A). The growth of MDA-MB-231 cells treated with 50 μM of **3**, **10**, and **13** was higher than that of A549 cells (Supplementary Figure S2B), which is consistent with difference in the KDM5A expression level between MDA-MB-231 and A549 cells. The results of cellular assays suggest that **10** and **13** inhibited KDM5s in A549 cells and induced cell growth inhibition.

4. Conclusion

In conclusion, to identify novel KDM5-selective inhibitors, we designed several compounds on the basis of our previous reports. By the inhibitor-based fragment merging strategy, i.e., the conjugation of an amino alkyl chain with a 3-cyano pyrazolo[1,5-*a*]pyrimidin-7-one scaffold, we identified **10** and **13**, which showed potent KDM5 inhibitory activity compared to the previously reported representative KDM5 inhibitor CPI-455 (**3**). In particular, **13** strongly inhibited KDM5A, KDM5B, and KDM5C, whereas **10** exhibited low KDM5C selectivity. In addition, both inhibitors showed high selectivity for the KDM5 subfamily over other KDMs. In cellular assays using A549 cells, compounds **10** and **13** increased H3K4me3 levels without affecting H3K9me3 and H3K27me3 levels, which indicates that **10** and **13** selectively inhibit KDM5s in cells. Compounds **10** and **13** also inhibited the growth of A549 cells more strongly than CPI-455 (**3**). We believe that the compounds described here will be useful tools for probing the biology of KDM5s and be candidate therapeutic agents for cancer, and the fragment merging strategy will be applied to other targets.

5. Experimental section

5.1. Chemistry

5.1.1. General

Reagents and solvents were purchased from Aldrich, Merck, Nacalai Tesque, Tokyo Kasei Kogyo, Wako Pure Chemical Industries, Kishida Kagaku, and Kanto Kagaku, and were used as received. Flash column chromatography was performed using silica gel supplied by Merck or Toyota Silica gel. Proton nuclear magnetic resonance spectra (^{1}H NMR) and carbon nuclear magnetic resonance spectra (^{13}C NMR) were recorded on a Bruker AVANCE 300 spectrometer in solvent as indicated. Chemical shifts (δ) are reported in parts per million relative to internal tetramethylsilane. Electrospray ionization (ESI) mass spectra were recorded on a Bruker HCTplus mass spectrometer or a Shimadzu LCMS-2020 instrument. High-resolution mass spectra (HRMS) were recorded on a Shimadzu LCMS-IT-TOF mass spectrometer. Melting points were determined using a Yanaco Micro Melting Point apparatus. The purity of all tested compounds was determined by HPLC using a Shimadzu UFLC system (SPDM20A UV detector, DGU-20A3R degassing unit, LC-20AD solvent delivery unit, and CBM-20A system) with a 5C18-AR-II column (150 mm × φ4.6 mm, Cosmosil) (UV detection, λ = 220 or 254 nm; flow, 1 mL/min). Microwave reactions were carried out in a Biotage microwave reaction kit (sealed vials) in an Initiator+ (Biotage).

5.1.2. Synthesis of 4′-((2-(hexyl(methyl)amino)ethyl)carbamoyl)-[2,2′-bipyridine]-4-carboxylic acid (7)

5.1.2.1. Preparation of 2-(2-(hexyl(methyl)amino)ethyl)isoindoline-1,3-dione (14). A solution of phthalimide (2.94 g, 20.0 mmol) in DMF (20 mL) was added to a suspension of 1,2-dibromoethane (1.85 mL, 29.6 mmol) and K_2CO_3 (5.52 g, 40.0 mmol) in DMF (40 mL) in a dropwise fashion, and the resulting suspension was stirred at room temperature for 2 h. Then, the reaction was quenched with water and extracted with *n*-hexane/AcOEt (2/1). The organic layer was separated and concentrated in vacuo. The residue was purified by silica gel column chromatography to give 2-(2-bromoethyl)isoindoline-1,3-dione (1.73 g, 34%). A mixture of 2-(2-bromoethyl)isoindoline-1,3-dione (158 mg, 0.624 mmol), *N*-hexylmethylamine (190 μL, 1.25 mmol), and K_2CO_3 (104 mg, 0.749 mmol) in DMF (1.5 mL) was stirred at 100 °C for 3 h. The reaction mixture was cooled and concentrated in vacuo. The residue was extracted with AcOEt, washed with water, and dried over Na_2SO_4. Filtration, evaporation in vacuo, and purification by silica gel column chromatography gave **14** (82.0 mg, 46%): ^{1}H NMR ($CDCl_3$, 300 MHz, δ; ppm), 7.85–7.68 (4H, m), 3.80 (2H, t, J = 6.6 Hz), 2.64 (2H, t, J = 6.6 Hz), 2.36 (2H, t, J = 7.5 Hz), 2.29 (3H, s), 1.37–1.17 (8H, m), 0.81 (3H, t, J = 6.3 Hz); ^{13}C NMR ($CDCl_3$, 75 MHz, δ; ppm), 168.4, 133.8, 132.2, 123.1, 57.8, 54.8, 42.2, 35.9, 31.7, 27.2, 27.0, 22.6, 14.0; MS (ESI) *m/z* 289.1 (MH^+).

5.1.2.2. Preparation of N^1-hexyl-N^1-methylethane-1,2-diamine (15). A solution of **14** (100 mg, 347 μmol) and $N_2H_4{\cdot}H_2O$ (35 μL, 270 μmol) in EtOH (3.0 mL) was heated at reflux temperature for 2 h. The reaction mixture was filtered and the filtrate was concentrated in vacuo. The residue was suspended in 5 mL of CH_2Cl_2 and the insoluble material was removed by filtration. The filtrate was concentrated to obtain **15** (50.0 mg, 91%): ^{1}H NMR ($CDCl_3$, 300 MHz, δ; ppm), 2.77 (2H, t, J = 6.0 Hz), 2.40 (2H, t, J = 6.0 Hz), 2.32 (2H, t, J = 7.5 Hz), 2.21 (3H, s), 1.79 (2H, br), 1.52–1.24 (8H, m), 0.88–0.94 (3H, m); ^{13}C NMR ($CDCl_3$, 75 MHz, δ; ppm), 60.6, 58.1, 54.1, 42.2, 39.6, 29.7, 27.0, 22.6, 14.0; MS (ESI) *m/z* 159.1 (MH^+).

5.1.2.3. Preparation of [2,2′-bipyridine]-4,4′-dicarboxylic acid (16). A solution of 4,4′-dimethyl-2,2′-bipyridine (1.02 g, 5.43 mmol) and potassium permanganate (3.20 g, 20.4 mmol) in H_2O (35 mL) was heated at reflux temperature for 6 h. The reaction mixture was filtered through Celite and ether was added to the residue to remove the unreacted starting material. The water layer was separated and acidified with 6 N aqueous HCl solution. The precipitate was collected by filtration and washed with water to give **16** (1.34 g, 99%) as a white powder: mp > 300 °C; ^{1}H NMR (DMSO-d_6, 300 MHz, δ; ppm), 8.92 (2H, d, J = 4.2 Hz), 8.85 (2H, s), 7.91 (2H, d, J = 3.3 Hz); ^{13}C NMR (DMSO-d_6, 75 MHz, δ; ppm), 166.5, 156.0, 151.1, 140.0, 123.9, 120.0; MS (ESI) *m/z* 244.1 (MH^+).

5.1.2.4. Preparation of dimethyl [2,2′-bipyridine]-4,4′-dicarboxylate (17). Thionyl chloride (300 μL, 4.08 mmol) was added to a suspension of **16** (400 mg, 1.62 mmol) in MeOH (30 mL) in a dropwise fashion. The mixture was heated at reflux temperature overnight. Then, the solvent was removed under reduced pressure and the residue was partitioned between CH_2Cl_2 and water. The organic layer was washed with saturated aqueous $NaHCO_3$ solution and dried over Na_2SO_4. Filtration, evaporation in vacuo, and recrystallization in AcOEt gave **17** (400 mg, 91%): mp 200–202 °C; ^{1}H NMR ($CDCl_3$, 300 MHz, δ; ppm), 8.92 (2H, d, J = 4.2 Hz), 8.85 (2H, s), 7.91 (2H, d, J = 3.3 Hz); ^{13}C NMR ($CDCl_3$, 75 MHz, δ; ppm), 166.5, 156.0, 151.1, 140.0, 123.9, 120.0; MS (ESI) *m/z* 273.0 (MH^+).

5.1.2.5. Preparation of 4′-(methoxycarbonyl)-[2,2′-bipyridine]-4-carboxylic acid (18). A solution of NaOH (27.0 mg, 0.488 mmol) in water (1 mL) was added to a solution of **17** (100 mg, 0.286 mmol) in MeOH/THF (5 mL/5 mL). The mixture was stirred at room temperature overnight. Then, the reaction mixture was concentrated in vacuo and the residue was extracted with water. The water layer was washed with AcOEt twice and acidified with 6 N aqueous HCl solution to adjust the pH to 2. The white precipitate was collected and dried in vacuo to give

18 (80.0 mg, 84%): mp > 300 °C; ^{1}H NMR (DMSO-d_6, 300 MHz, δ; ppm), 8.92 (2H, m), 8.85 (2H, s), 7.93 (2H, m), 3.96 (3H, s); ^{13}C NMR (DMSO-d_6, 75 MHz, δ; ppm), 166.6, 165.6, 156.2, 156.0, 151.4, 151.3, 140.2, 138.9, 124.2, 124.1, 120.2, 119.9, 53.52; MS (ESI) *m/z* 258.2 (MH^+).

*5.1.2.6. Preparation of methyl 4′-((2-(hexyl(methyl)amino)ethyl) carbamoyl)-[2,2′-bipyridine]-4-carboxylate (**19**)*. A solution of Et_3N (20.0 μL, 0.146 mmol) and EDCI·HCl (28.0 mg, 0.146 mmol) in DMF (1 mL) was added to a solution of **18** (40.0 mg, 0.146 mmol), **15** (25.0 mg, 0.158 mmol), and HOBt (22.0 mg, 0.158 mmol) in DMF (5 mL). The mixture was stirred at room temperature overnight. Then, the solvent was removed under reduced pressure and the residue was extracted with AcOEt. The organic layer was washed with water and dried over Na_2SO_4. Filtration, evaporation in vacuo, and purification by silica gel column chromatography gave **19** (7.02 mg, 12%): mp 86.5–88.0 °C; ^{1}H NMR ($CDCl_3$, 300 MHz, δ; ppm), 8.95 (2H, m), 8.84 (2H, s), 7.91–7.84 (2H, m), 4.01 (3H, s), 3.76 (2H, t, J = 6.0 Hz), 3.00 (2H, t, J = 4.5 Hz), 2.76 (2H, t, J = 7.5 Hz), 2.60 (2H, s), 1.34–1.27 (8H, m), 0.87 (3H, t, J = 6.9 Hz); ^{13}C NMR ($CDCl_3$, 75 MHz, δ; ppm): 165.8, 165.7, 156.6, 156.3, 150.2, 150.1, 142.3, 138.5, 123.1, 121.7, 120.6, 118.6, 57.63, 53.04, 52.68, 41.40, 36.27, 31.39, 29.68, 26.64, 22.43, 13.88; MS (ESI) *m/z* 399.3 (MH^+).

*5.1.2.7. Preparation of 4′-((2-(hexyl(methyl)amino)ethyl)carbamoyl)-[2,2′-bipyridine]-4-carboxylic acid (**7**)*. A 6 N aqueous NaOH solution (7.00 μL, 0.420 mmol) was added to a solution of **19** (5.00 mg, 13.0 μmol) in MeOH (1 mL). The mixture was stirred at room temperature overnight. The reaction mixture was concentrated in vacuo and the residue was acidified with 4 N HCl in dioxane (1 mL). Then, the insoluble materials were removed by filtration and the filtrate was concentrated in vacuo to give **7** (3.00 mg, 60%): mp 135–137 °C; ^{1}H NMR (DMSO-d_6, 300 MHz, δ; ppm), 9.39 (1H, s), 8.88 (2H, q, J = 5.1 Hz), 8.83 (2H, s), 7.99 (1H, d, J = 4.8 Hz), 7.91 (1H, d, J = 4.8 Hz), 3.71 (2H, t, J = 4.8 Hz), 3.03 (2H, t, J = 7.5 Hz), 2.77 (3H, s), 1.67–1.65 (2H, m), 1.25–1.18 (8H, m), 0.83 (3H, t, J = 6.9 Hz); ^{13}C NMR (DMSO-d_6, 75 MHz, δ; ppm), 165.5, 155.8, 155.7, 150.7, 150.6, 142.3, 138.5, 124.1, 122.4, 120.3, 118.9, 55.59, 54.15, 45.60, 31.18, 26.16, 23.60, 22.31, 14.24; MS (ESI) *m/z* 385.2 (MH^+); HRMS (ESI) calcd for $C_{21}H_{29}N_4O_3^+$, 385.2234, found, 385.2237; HPLC t_R = 10.58 min, purity 96.6% (HPLC conditions, eluent A: H_2O containing 0.1% TFA, eluent B: acetonitrile containing 0.1% TFA. Gradient, B: 0 to 20 min, 10–90%, 20 to 30 min, 90%).

*5.1.3. Synthesis of 2-((3-(hexyl(methyl)amino)propyl)carbamoyl) isonicotinic acid (**8**)*

*5.1.3.1. Preparation of 2-(3-(hexyl(methyl)amino)propyl)isoindoline-1,3-dione (**20**)*. A mixture of *N*-(3-bromopropyl)phthalimide (268 mg, 1.0 mmol), K_2CO_3 (207 mg, 1.5 mmol), and *N*-hexylmethylamine (0.17 mL, 1.1 mmol) in MeCN (5 mL) was heated at reflux temperature for 1 h. Filtration, evaporation in vacuo, and purification by flash column chromatography gave **20** (255 mg, 84%): ^{1}H NMR (DMSO-d_6, 300 MHz, δ; ppm), 7.88–7.79 (4H, m), 3.59 (2H, t, J = 6.9 Hz), 2.29 (2H, t, J = 6.9 Hz), 2.19 (2H, t, J = 6.9 Hz), 2.05 (3H, s), 1.75–1.66 (2H, m), 1.28–1.19 (8H, m), 0.83 (3H, t, J = 6.9 Hz).

*5.1.3.2. Preparation of N^1-hexyl-N^1-methylpropane-1,3-diamine (**21**)*. Compound **21** was prepared from **20** by using a similar procedure to the one used for the preparation of **15**. Yield, 107 mg, 75%; ^{1}H NMR (DMSO-d_6, 300 MHz, δ; ppm), 2.52 (2H, t, J = 7.2 Hz), 2.26 (2H, t, J = 7.2 Hz), 2.21 (2H, t, J = 7.2 Hz), 2.07 (3H, s), 1.48–1.34 (4H, m), 1.24 (6H, brs), 0.83 (3H, t, J = 6.6 Hz).

*5.1.3.3. Preparation of dimethyl pyridine-2,4-dicarboxylate (**22**)*. Compound **22** was prepared from 2,4-pyridinedicarboxylic acid by using a similar procedure to the one used for the preparation of **17**. Yield, 1.74 g, 89%; ^{1}H NMR (DMSO-d_6, 300 MHz, δ; ppm), 8.93 (1H, dd, J = 6.9, 0.6 Hz), 8.383–8.378 (1H, m), 8.07 (1H, dd, J = 6.9, 1.5 Hz), 3.93 (3H, s), 3.92 (3H, s).

*5.1.3.4. Preparation of methyl 2-((3-(hexyl(methyl)amino)propyl) carbamoyl)isonicotinate (**24**)*. A mixture of **22** (137 mg, 0.70 mmol) and KOH (43.2 mg, 0.77 mmol) in MeOH (2 mL) was heated at reflux temperature for 1 h. Then, the reaction mixture was concentrated in vacuo to give crude **23**. Crude **23** was dissolved in DMF (2 mL) and a solution of **21** in DMF (2 mL), Et_3N (0.24 mL, 1.75 mmol), EDCI·HCl (148 mg, 0.77 mmol), and HOBt (104 mg, 0.77 mmol) were added. The resulting mixture was heated at 70 °C for 4.5 h. The reaction was quenched with water and extracted with AcOEt. The organic layer was separated and dried over Na_2SO_4. Filtration, evaporation in vacuo, and purification by silica gel column chromatography gave **24** (66 mg, 32%): ^{1}H NMR (DMSO-d_6, 300 MHz, δ; ppm), 8.99 (1H, t, J = 5.1 Hz), 8.85 (1H, dd, J = 5.1, 0.6 Hz), 8.40 (1H, s), 7.98 (1H, dd, J = 8.1, 1.8 Hz), 3.91 (3H, s), 3.26 (2H, m), 2.33 (2H, t, J = 6.9 Hz), 2.25 (2H, t, J = 6.9 Hz), 2.12 (3H, s), 1.71–1.62 (2H, m), 1.36–1.34 (2H, m), 1.21 (6H, s), 0.82 (3H, t, J = 6.9 Hz).

*5.1.3.5. Preparation of 2-((3-(hexyl(methyl)amino)propyl)carbamoyl) isonicotinic acid (**8**)*. A mixture of **24** (65 mg, 0.19 mmol) and KOH (25.1 mg, 0.38 mmol) in MeOH (3 mL) was heated at reflux temperature for 1 h. The reaction mixture was concentrated in vacuo and purified by silica gel column chromatography to give **8** (53 mg, 87%): mp 137–140 °C; ^{1}H NMR (DMSO-d_6, 300 MHz, δ; ppm), 9.01 (1H, t, J = 5.4 Hz), 8.60 (1H, d, J = 4.8 Hz), 8.30 (1H, s), 7.65 (1H, dd, J = 5.4, 1.8 Hz), 3.29 (3H, q, J = 5.4 Hz), 2.46 (2H, m), 2.41 (3H, t, J = 7.5 Hz), 2.24 (3H, s), 1.77–1.68 (2H, m), 1.42 (2H, m), 1.21 (6H, brs), 0.82 (3H, t, J = 6.9 Hz); ^{13}C NMR (DMSO-d_6, 75 MHz, δ; ppm), 167.8, 165.3, 149.3, 142.0, 126.1, 121.5, 121.1, 57.41, 55.17, 42.13, 38.19, 31.62, 26.95, 26.76, 26.70, 22.51, 14.35; LC-MS (ESI) *m/z* 321 (MH^+); HRMS (ESI) calcd for $C_{17}H_{28}N_3O_3^+$, 322.2125, found, 322.2123; HPLC t_R = 8.93 min, purity 98.3% (HPLC conditions, eluent A: H_2O containing 0.1% TFA, eluent B: acetonitrile containing 0.1% TFA. Gradient, B: 0 to 20 min, 10–90%, 20 to 30 min, 90%).

*5.1.4. Synthesis of 2-(4-(3-(hexyl(methyl)amino)propyl)-2,3-dioxo-3,4-dihydroquinoxalin-1(2H)-yl)acetic acid (**9**)*

*5.1.4.1. Preparation of ethyl 2-(2,3-dioxo-3,4-dihydroquinoxalin-1(2H)-yl)acetate (**25**)*. 60% NaH in oil (88 mg, 2.2 mmol) was added to a solution of quinoxaline-2,3-dione (324 mg, 2.0 mmol) in DMF (20 mL) with cooling in an ice bath. Then, ethyl bromoacetate (0.21 mL, 1.9 mmol) was also added to the mixture and the resulting mixture was stirred at room temperature for 2 h. The reaction was quenched with water and extracted with AcOEt. The organic layer was washed with brine and dried over Na_2SO_4. Filtration and evaporation in vacuo gave a crude solid. The crude solid was suspended in $CHCl_3$ (5 mL) and the insoluble material was collected by filtration to give **25** (117 mg, 25%): ^{1}H NMR (DMSO-d_6, 300 MHz, δ; ppm), 12.20 (1H, brs), 7.31–7.28 (1H, m), 7.23–7.14 (3H, m), 4.97 (2H, s), 4.16 (2H, q, J = 7.2 Hz), 1.21 (3H, t, J = 7.2 Hz).

*5.1.4.2. Preparation of ethyl 2-(4-(3-chloropropyl)-2,3-dioxo-3,4-dihydroquinoxalin-1(2H)-yl)acetate (**26**)*. 60% NaH in oil (22 mg, 0.55 mmol) was added to a solution of **25** (115 mg, 0.46 mmol) in DMF (5 mL) with cooling in an ice bath. Then, 1-bromo-3-chloropropane (0.09 mL, 0.92 mmol) was added to the mixture and the resulting mixture was stirred at room temperature for 2 h. The reaction was quenched with water and extracted with AcOEt. The organic layer was washed with brine and dried over Na_2SO_4. Filtration, evaporation in vacuo, and purification by flash column chromatography gave **26** (81 mg, 54%): ^{1}H NMR (DMSO-d_6, 300 MHz, δ; ppm), 7.52 (1H, dd, J = 8.1, 1.2 Hz), 7.38–7.23 (3H, m), 5.00 (2H, s), 4.28 (2H, t, J = 7.5 Hz), 4.17 (2H, q, J = 7.2 Hz), 3.79

(2H, t, J = 6.6 Hz), 2.15–2.04 (2H, m), 1.21 (3H, t, J = 7.2 Hz).

*5.1.4.3. Preparation of ethyl 2-(4-(3-(hexyl(methyl)amino)propyl)-2,3-dioxo-3,4-dihydroquinoxalin-1(2H)-yl)acetate (**27**)*. Compound **27** was prepared from **26** by using a similar procedure to the one used for the preparation of **20**. Yield, 83 mg, 82%; ^{1}H NMR (DMSO-d_6, 300 MHz, δ; ppm), 7.54 (1H, dd, J = 8.1, 1.5 Hz), 7.36 (1H, dd, J = 7.5, 1.8 Hz), 7.28 (2H, td, J = 7.5, 1.8 Hz), 5.00 (2H, s), 4.20–4.13 (4H, m), 3.30–3.26 (2H, m), 2.39 (2H, t, J = 7.5 Hz), 2.26 (3H, t, J = 7.5 Hz), 1.77 (2H, t, J = 7.5 Hz), 1.40 (2H, m), 1.25 (6H, m), 1.21 (3H, t, J = 7.5 Hz), 0.85 (3H, t, J = 6.9 Hz).

*5.1.4.4. Preparation of 2-(4-(3-(hexyl(methyl)amino)propyl)-2,3-dioxo-3,4-dihydroquinoxalin-1(2H)-yl)acetic acid hydrochloride (**9**·HCl)*. To a solution of **27** (81 mg, 0.2 mmol) in THF/H_2O (1.5 mL/1.5 mL) was added NaOH (16 mg, 0.4 mmol) and the mixture was stirred at room temperature for 2 h. Then, the reaction mixture was acidified with 1 N aqueous HCl solution to adjust the pH to 3, and concentrated in vacuo. The residue was purified by flash column chromatography to obtain a solid. The solid was dissolved in 4 N HCl in AcOEt and concentrated in vacuo. The residue was suspended in Et_2O and the insoluble material was collected by filtration to give **9** (56 mg, 75%): mp 110–112 °C; ^{1}H NMR (DMSO-d_6, 300 MHz, δ; ppm), 7.49–7.46 (1H, m), 7.29–7.20 (3H, m), 4.46 (2H, s), 4.18–4.11 (2H, m), 2.57–2.56 (2H, m), 2.32 (3H, m), 2.17 (2H, s), 1.77 (2H, m), 1.42 (2H, s), 1.26 (6H, m), 0.85 (3H, m); ^{13}C NMR (DMSO-d_6, 75 MHz, δ; ppm), 169.1, 154.1, 154.0, 127.2, 126.4, 124.6, 124.5, 115.9, 55.40, 52.77, 44.80, 31.10, 26.04, 23.59, 22.26, 21.98, 21.30, 14.23; LC-MS (ESI) m/z 375 (MH^+-HCl); HRMS (ESI) calcd for $C_{20}H_{30}N_3O_4^+$, 376.2231, found, 376.2235; HPLC t_R = 10.6 min, purity 98.8% (HPLC conditions, eluent A: H_2O containing 0.1% TFA, eluent B: acetonitrile containing 0.1% TFA. Gradient, B: 0 to 20 min, 10–90%, 20 to 30 min, 90%).

*5.1.5. Synthesis of 5-(4-((hexyl(methyl)amino)methyl)phenyl)-6-isopropyl-7-oxo-4,7-dihydropyrazolo[1,5-a]pyrimidine-3-carbonitrile (**10**)*

*5.1.5.1. Preparation of 6-isopropyl-5,7-dioxo-4,5,6,7-tetrahydropyrazolo [1,5-a]pyrimidine-3-carbonitrile (**28**)*. A solution of diethyl isopropylmalonate (2.1 mL, 10 mmol), 3-amino-4-pyrazolecarbonitrile (1.1 g, 10 mmol), and NaOEt (20% in EtOH, 10 mL) in EtOH (5 mL) was heated by MW at 160 °C for 0.5 h. MeOH was added to the reaction mixture and the reaction mixture was acidified with 4 N HCl in AcOEt to adjust the pH to 1. The precipitate was collected by filtration and washed with Et_2O to give **28** (2.18 g, quant.): ^{1}H NMR (DMSO-d_6, 300 MHz, δ; ppm), 8.21 (1H, s), 3.21 (1H, m), 1.21 (6H, d, J = 6.6 Hz).

*5.1.5.2. Preparation of 5-chloro-6-isopropyl-7-oxo-4,7-dihydropyrazolo [1,5-a]pyrimidine-3-carbonitrile (**29**)*. A solution of **28** (1.09 g, 5.0 mmol) in $POCl_3$ (20 mL) was heated by MW at 170 °C for 2 h. Then, the reaction was quenched with water and extracted with AcOEt. The organic layer was separated and dried over Na_2SO_4, Filtration, evaporation in vacuo, and purification by silica gel column chromatography gave the dichloro intermediate (335 mg, 26%). A solution of the intermediate (335 mg, 1.31 mmol) and 1 N aqueous NaOH solution (2.6 mL, 2.6 mmol) in THF (2.6 mL) was heated at reflux temperature for 0.75 h. Then, the reaction was quenched with 4 N HCl in AcOEt to adjust the pH to 1 and extracted with AcOEt. The organic layer was separated and dried over Na_2SO_4, and this was followed by filtration and evaporation in vacuo. The residue was collected by filtration and washed with n-hexane/AcOEt (1/9) to give **29** (224 mg, 72%): ^{1}H NMR (DMSO-d_6, 300 MHz, δ; ppm), 8.20 (1H, s), 3.27 (1H, m), 1.28 (6H, d, J = 6.9 Hz).

*5.1.5.3. Preparation of N-methyl-N-(4-(4,4,5,5-tetramethyl-1,3,2-dioxaborolan-2-yl)benzyl)hexan-1-amine (**32a**)*. Compound **32a** was prepared from 2-(4-(bromomethyl)phenyl)-4,4,5,5-tetramethyl-1,3,2-dioxaborolane by using a similar procedure to the one used for the preparation of **20**. Yield, 694 mg, 69%; ^{1}H NMR ($CDCl_3$, 300 MHz, δ; ppm), 7.78 (2H, d, J = 7.8 Hz), 7.34 (2H, d, J = 7.8 Hz), 3.51 (2H, s), 2.20 (3H, s), 1.57–1.47 (2H, m), 1.36 (12H, s), 1.33–1.28 (6H, m), 1.28 (2H, t, J = 7.2 Hz), 0.90 (3H, t, J = 6.9 Hz).

*5.1.5.4. Preparation of 5-(4-((hexyl(methyl)amino)methyl)phenyl)-6-isopropyl-7-oxo-4,7-dihydropyrazolo[1,5-a]pyrimidine-3-carbonitrile (**10**)*. A solution of **29** (118 mg, 0.50 mmol), **32a** (182 mg, 0.55 mmol), Na_2CO_3 (106 mg, 1.0 mmol), and $PdCl_2(dppf)\cdot CH_2Cl_2$ (37 mg, 0.050 mmol) in DME/H_2O (3 mL/1 mL) was heated by MW at 160 °C for 0.5 h. After the reaction mixture was filtered, the filtrate was extracted with AcOEt and washed with brine. The organic layer was separated and dried over Na_2SO_4. Filtration, evaporation in vacuo, and purification by silica gel column chromatography gave a crude solid. The crude solid was recrystallized in MeOH to give **10** (41 mg, 20%): mp 228–230 °C; ^{1}H NMR (DMSO-d_6, 300 MHz, δ; ppm), 8.07 (1H, s), 7.53 (2H, d, J = 7.8 Hz), 7.44 (2H, d, J = 7.8 Hz), 4.23 (2H, brs), 2.98 (2H, brs), 2.69–2.65 (4H, m), 1.65 (2H, m), 1.28–1.23 (12H, m), 0.87 (3H, t, J = 6.6 Hz); ^{13}C NMR (DMSO-d_6, 75 MHz, δ; ppm), 157.5, 148.5, 132.4, 131.3, 130.7, 128.9, 114.2, 111.2, 108.4, 98.15, 74.63, 57.12, 56.02, 31.21, 29.27, 26.98, 26.24, 25.41, 22.34, 20.98, 14.29; LC-MS (ESI) m/z 405 (MH^+); HRMS (ESI) calcd for $C_{24}H_{32}N_5O^+$, 406.2601, found, 406.2605; HPLC t_R = 13.10 min, purity 97.1% (HPLC conditions, eluent A: H_2O containing 0.1% TFA, eluent B: acetonitrile containing 0.1% TFA. Gradient, B: 0 to 20 min, 10–90%, 20 to 30 min, 90%).

*5.1.6. Synthesis of 5-(3-((hexyl(methyl)amino)methyl)phenyl)-6-isopropyl-7-oxo-4,7-dihydropyrazolo[1,5-a]pyrimidine-3-carbonitrile (**11**)*

*5.1.6.1. Preparation of N-methyl-N-(3-(4,4,5,5-tetramethyl-1,3,2-dioxaborolan-2-yl)benzyl)hexan-1-amine (**32b**)*. Compound **32b** was prepared from 2-(3-(bromomethyl)phenyl)-4,4,5,5-tetramethyl-1,3,2-dioxaborolane by using a similar procedure to the one used for the preparation of **20**. Yield, 542 mg, 82%; ^{1}H NMR (DMSO-d_6, 300 MHz, δ; ppm), 7.62 (1H, s), 7.54 (1H, d, J = 7.2 Hz), 7.40 (1H, d, J = 7.2 Hz), 7.32 (1H, t, J = 7.2 Hz), 3.43 (2H, s), 2.29 (2H, t, J = 7.2 Hz), 2.08 (3H, s), 1.46–1.16 (8H, m), 1.28–1.23 (12H, m), 0.85 (3H, t, J = 6.9 Hz).

*5.1.6.2. Preparation of 5-(3-((hexyl(methyl)amino)methyl)phenyl)-6-isopropyl-7-oxo-4,7-dihydropyrazolo[1,5-a]pyrimidine-3-carbonitrile (**11**)*. Compound **11** was prepared from **29** and **32b** by using a similar procedure to the one used for the preparation of **10**. Yield, 30 mg, 7%; mp 272–274 °C; ^{1}H NMR (DMSO-d_6, 300 MHz, δ; ppm), 8.08 (1H, s), 7.53–7.41 (4H, m), 4.27 (2H, brs), 2.97 (2H, brs), 2.64 (3H, brs), 1.65 (2H, brs), 1.26–1.22 (13H, m), 0.86 (3H, t, J = 6.9 Hz); ^{13}C NMR (DMSO-d_6, 75 MHz, δ; ppm), 157.1, 144.6, 130.7, 130.6, 130.3, 129.8, 129.2, 128.7, 115.6, 111.6, 86.25, 81.41, 74.57, 59.36, 55.53, 31.16, 29.28, 26.23, 24.20, 22.31, 20.93, 14.25; LC-MS (ESI) m/z 405 (M^+); HRMS (ESI) calcd for $C_{24}H_{31}N_5O^+$, 406.2601, found, 406.2597; HPLC t_R = 13.1 min, purity 99.3% (HPLC conditions, eluent A: H_2O containing 0.1% TFA, eluent B: acetonitrile containing 0.1% TFA. Gradient, B: 0 to 20 min, 10–90%, 20 to 30 min, 90%).

*5.1.7. Synthesis of 5-(5-((hexyl(methyl)amino)methyl)thiophen-2-yl)-6-isopropyl-7-oxo-4,7-dihydropyrazolo[1,5-a]pyrimidine-3-carbonitrile (**12**)*

*5.1.7.1. Preparation of N-((4-bromothiophen-2-yl)methyl)-N-methylhexan-1-amine (**31a**)*. A solution of 4-bromothiophene-2-carboxyaldehyde (1.15 g, 6.0 mmol), *N*-hexylmethylamine (0.76 mL, 5.0 mmol), and $NaBH(OAc)_3$ (1.86 g, 7.0 mmol) in 1,2-DCE (30 mL) was stirred at room temperature for 5 h. The reaction was quenched with water and extracted with $CHCl_3$. The organic layer was separated, washed with brine, and dried over Na_2SO_4. Filtration, evaporation in vacuo, and purification by silica gel column chromatography gave **31a** (0.92 g, 53%): ^{1}H NMR (DMSO-d_6, 300 MHz, δ; ppm), 7.54 (1H, d, J = 1.5 Hz), 6.96 (1H, d, J = 1.5 Hz), 3.64 (2H, s), 2.32 (2H, d, J = 6.9 Hz), 2.16 (3H, s), 1.45–1.38 (2H, m), 1.31–1.24 (6H, m), 0.86

(3H, t, J = 6.9 Hz).

*5.1.7.2. Preparation of N-((4-bromothiophen-2-yl)methyl)-N-methylhexan-1-amine (**32c**).* A mixture of **31a** (871 mg, 3.0 mmol), bis(pinacolate)diboron (1.1 g, 4.5 mmol), AcOK (441 mg, 4.5 mmol), and $PdCl_2(dppf)\cdot CH_2Cl_2$ (112 mg, 0.15 mmol) in dioxane (9 mL) was heated by MW at 140 °C for 0.5 h. The reaction mixture was filtered through Celite and the solvent was removed under reduced pressure. The residue was purified by silica gel column chromatography to give crude **32c** (266 mg), which was used in the next step without further purification.

*5.1.7.3. Preparation of 5-(5-((hexyl(methyl)amino)methyl)thiophen-3-yl)-6-isopropyl-7-oxo-4,7-dihydropyrazolo[1,5-a]pyrimidine-3-carbonitrile (**12**).* Compound **12** was prepared from **29** and **32c** by using a similar procedure to the one used for the preparation of **10**. Yield, 65 mg, 20%; mp 173–175 °C; ^{1}H NMR (DMSO-d_6, 300 MHz, δ; ppm), 8.08 (1H, s), 7.56–7.41 (2H, m), 4.27 (2H, brs), 2.98 (2H, brs), 2.65 (3H, s), 1.65 (2H, brs), 1.26–1.22 (13H, m), 0.86 (3H, t, J = 6.9 Hz); ^{13}C NMR (DMSO-d_6, 75 MHz, δ; ppm), 159.7, 156.9, 144.8, 141.1, 138.2, 129.6, 126.7, 123.8, 116.2, 112.3, 74.60, 55.51, 54.07, 31.27, 29.08, 26.38, 24.95, 22.39, 21.02, 14.29; MS (ESI) m/z 411 (MH^+); HRMS (ESI) calcd for $C_{22}H_{30}N_5OS^+$, 412.2166, found, 412.2161; HPLC t_R = 12.9 min, purity 95.7% (HPLC conditions, eluent A: H_2O containing 0.1% TFA, eluent B: acetonitrile containing 0.1% TFA. Gradient, B: 0 to 20 min, 10–90%, 20 to 30 min, 90%).

*5.1.8. Synthesis of 5-(4-(2-(hexyl(methyl)amino)ethyl)phenyl)-6-isopropyl-7-oxo-4,7-dihydropyrazolo[1,5-a]pyrimidine-3-carbonitrile (**13**)*

*5.1.8.1. Preparation of 2-(4-bromophenyl)acetaldehyde (**30**).* A solution of 2-(4-bromophenyl)ethyl alcohol (2.00 g, 10.0 mmol) and Dess-Martin periodinane (4.20 g, 12.0 mmol) in CH_2Cl_2 (100 mL) was stirred at room temperature for 1 h. The reaction was quenched with 1 M aqueous $Na_2S_2O_3$ solution and extracted with CH_2Cl_2. The organic layer was separated, washed with brine, and dried over Na_2SO_4, Filtration, evaporation in vacuo, and purification by silica gel column chromatography gave **30** (1.23 g, 62%): ^{1}H NMR (DMSO-d_6, 300 MHz, δ; ppm), 9.68 (1H, t, J = 1.5 Hz), 7.56–7.52 (2H, m), 7.22–7.18 (2H, m), 3.79 (2H, d, J = 1.5 Hz).

*5.1.8.2. Preparation of N-(4-bromophenethyl)-N-methylhexan-1-amine (**31b**).* Compound **31b** was prepared from **30** by using a similar procedure to the one used for the preparation of **31a**. Yield, 1.46 g, 79%; ^{1}H NMR (DMSO-d_6, 300 MHz, δ; ppm), 7.48–7.44 (2H, m), 7.22–7.18 (2H, m), 2.72–2.67 (4H, m), 2.45 (2H, m), 2.29 (3H, s), 1.42–1.38 (2H, m), 1.26–1.15 (6H, m), 0.85 (3H, t, J = 6.9 Hz).

*5.1.8.3. Preparation of N-methyl-N-(4-(4,4,5,5-tetramethyl-1,3,2-dioxaborolan-2-yl)phenethyl)hexan-1-amine (**32d**).* Compound **32d** was prepared from **31b** by using a similar procedure to the one used for the preparation of **32c**. Yield, 0.88 g, 85%; ^{1}H NMR (DMSO-d_6, 300 MHz, δ; ppm), 7.57 (2H, d, J = 8.1 Hz), 7.22 (2H, d, J = 8.1 Hz), 2.70 (2H, t, J = 7.2 Hz), 2.30 (2H, t, J = 7.2 Hz), 2.18 (3H, s), 1.37–1.15 (16H, m), 1.07 (6H, s), 0.85 (3H, t, J = 6.9 Hz).

*5.1.8.4. Preparation of 5-(4-(2-(hexyl(methyl)amino)ethyl)phenyl)-6-isopropyl-7-oxo-4,7-dihydropyrazolo[1,5-a]pyrimidine-3-carbonitrile (**13**).* Compound **13** was prepared from **29** and **32d** by using a similar procedure to the one used for the preparation of **10**. Yield, 77 mg, 18%; mp 184–186 °C; ^{1}H NMR (DMSO-d_6, 300 MHz, δ; ppm), 7.34–7.29 (4H, m), 3.34 (2H, m), 3.05–2.99 (4H, m), 2.75–2.68 (4H, s), 1.64 (2H, m), 1.29–1.23 (12H, m), 0.87 (3H, t, J = 6.9 Hz); ^{13}C NMR (DMSO-d_6, 75 MHz, δ; ppm), 158.6, 144.4, 128.8, 128.7, 128.6, 128.5, 114.4, 111.2, 107.0, 104.0, 74.60, 60.96, 56.96, 55.86, 31.22, 29.27, 26.23, 24.16, 22.36, 21.02, 14.30; MS (ESI) m/z 419 (MH^+); HRMS (ESI) calcd for $C_{25}H_{34}N_5O^+$, 420.2758, found, 420.2755; HPLC t_R = 13.61 min, purity 99.1% (HPLC conditions, eluent A: H_2O containing 0.1% TFA, eluent B: acetonitrile containing 0.1% TFA. Gradient, B: 0 to 20 min, 10–90%, 20 to 30 min, 90%).

5.2. Molecular docking

Docking study was performed using Molegro Virtual Docker 6.0 software. The structure of **13** bound to KDM5A (PDB code: 5CEH) was constructed by MolDock, which is based on a heuristic search algorithm that combines differential evolution with a cavity prediction algorithm. The docking parameters were as follows: grid resolution: 0.30, max iterations: 1500, population size: 50, energy threshold: 100.00, simplex evolution: 300 (max steps) and 1.00 (neighbor distance factor), search space: (X, Y, Z) = (130.00, 136.00, 110.00) with radius 15, distance constraints: an N atom of cyano group of **13** as an Fe(II) chelator, constraint center (X, Y, Z) = (131.49, 368.84, 109.93) with hard constraint between minimum 0.0 to maximum 0.5.

5.3. Enzyme assay

NCDM-81a (**1a**) and CPI-455 (**3**) were prepared according to the procedures reported by Itoh *et al.*[44] and Vinogradova *et al.*,[45] respectively. KDM activity assays were performed by an AlphaLISA screen assay system. All components are summarized in Supplementary Table S1. Initially, 2.5 μL of assay buffer (50 mM HEPES pH 7.5, 0.1% w/v BSA, 0.01% v/v Tween 20 containing 3% DMSO as control or blank) or 100X concentrated inhibitor solution (in assay buffer containing 3% DMSO) was introduced into the corresponding wells of a white opaque OptiPlate™-384. Then, 5.0 μL of enzyme solution was added to each well (For blank, 5.0 μL of assay buffer was added instead.). After that, 2.5 μL of peptide/2-OG (50 μM)/Fe(II) (5 μM)/Asc (100 μM) mix in assay buffer was added to each well. The final concentrations of enzyme and peptide substrate are summarized in Supplementary Table S2. The mixture was incubated for 1 h at room temperature with gentle shaking (250 rpm) (Protein A acceptor beads were pre-incubated with anti-methyl mark antibody for 1 h prior to addition to the assay plate.). Then, 5.0 μL of acceptor beads in epigenetic buffer (100 μg/mL) was added to each well and incubation was carried out for 1 h at room temperature with gentle shaking (250 rpm). Ten μL of donor beads in epigenetic buffer (50 μg/mL) was added to each well and incubation was carried out for 30 min at room temperature in the dark. Then, the Alpha signal of the wells was measured by an Ensight® reader from PerkinElmer Ltd. with excitation set at 615 nm and emission detection, at 655 nm, and % inhibition was calculated from the Alpha signal readings of inhibited wells relative to those of control wells. The concentration of a compound that results in 50% inhibitory concentration (IC_{50}) was determined by plotting log[Inh] versus the logit function of % inhibition. IC_{50} values were determined by regression analysis of the concentration/inhibition data. For determination of IC_{50} values, at least five concentrations of inhibitors were used.

5.4. Cellular assay

5.4.1. Cell cultures

Human lung cancer A549 cells (provided by RIKEN BRC through the National Bio-Resource Project of MEXT, Japan) were cultured in RPMI1640 containing 10% heat-inactivated fetal bovine serum (FBS), penicillin, and streptomycin mixture at 37 °C in a humidified atmosphere of 5% CO_2 in air. Human breast cancer MDA-MB-231 cells (provided by American type culture collection, ATCC, USA) were cultured in Leibovitz's L-15 medium containing 2 mM of glutamine, 10% FBS, and a penicillin and streptomycin mixture at 37 °C.

5.4.2. Western blot analysis

A549 and MDA-MB-231 cells (5×10^5 cells/2 mL/well) were treated for 48 h with the test compounds at the indicated concentrations

in the culture medium. The cells were collected and extracted with SDS buffer. Protein concentrations of the lysates were determined using a BCA protein assay. The equivalent amounts of protein from each lysate were resolved in 5–20% SDS-polyacrylamide gels and transferred onto PVDF membranes. After blocking with TBS-T containing 5% skimmed milk, the transblotted membranes were probed with primary antibodies (See Supplementary Table S3). The probed membranes were washed three times with TBS-T, incubated with HRP-linked secondary antibody (See Supplementary Table S3), and again washed three times with TBS-T. The immunoblots were visualized by enhanced chemiluminescence with chemiluminescent HRP substrate (See Supplementary Table S3).

5.4.3. Growth inhibition assay

A549 and MDA-MB-231 cells were plated in 96-well plates at the initial density of 2×10^3 cells per well (50 µL per well) and incubated at 37 °C. After 24 h, cells were exposed to the test compounds by adding solutions (50 µL per well) of the compounds at various concentrations in a medium at 37 °C under 5% CO_2 in air for 72 h. The mixtures were treated with 10 µL of AlamarBlue® (AbD Serotec, #BUF012A), and incubation was continued at 37 °C for 3 h. The fluorescence in each well was measured with an ARVO™ X3 microplate reader (excitation at 540 nm, emission at 590 nm). Percentage cell growth was calculated from the fluorescence readings.

Acknowledgments

The authors would like to thank Prof. K. Akaji and Dr. Y. Hattori for technical support in HRMS analysis. This work was supported by the JST CREST program (JPMJCR14L2 to T. Suzuki).

Appendix A. Supplementary data

Supplementary data to this article can be found online at https://doi.org/10.1016/j.bmc.2019.02.006.

References

1. Kouzarides T. *Cell.* 2007;128:693–705.
2. Huang H, Sabari BR, Garcia BA, Allis CD, Zhao Y. *Cell.* 2014;159:458.
3. Zhao S, Zhang X, Li H. *Curr Opin Struct Biol.* 2018;53:169–177.
4. Jenuwein T. *Science.* 2001;293:1074–1080.
5. Koprinarova M, Schnekenburger M, Diederich M. *Curr Top Med Chem.* 2016;16:732–744.
6. Bhanu NV, Sidoli S, Garcia BA. *Proteomics.* 2016;16:448–458.
7. Itoh Y, Suzuki T, Miyata N. *Mol Biosyst.* 2013;9:873–896.
8. Shanmugam MK, Arfuso F, Arumugam S, et al. *Oncotarget.* 2017;9:11414–11426.
9. Morera L, Lübbert M, Jung M. *Clin Epigenetics.* 2016;8:57.
10. Ganesan A. *ChemMedChem.* 2016;11:1227–1241.
11. Ota Y, Suzuki T. *Chem Rec.* 2018;18:1782–1791.
12. Itoh Y. *Chem Rec.* 2018;18:1681–1700.
13. Suzuki T, Miyata N. *J Med Chem.* 2011;54:8236–8250.
14. Shi Y. *Nat Rev Genet.* 2007;8:829–833.
15. Kooistra SM, Helin K. *Nat Rev Mol Cell Biol.* 2012;13:297–311.
16. Burg JM, Link JE, Morgan BS, Heller FJ, Hargrove AE, McCafferty DG. *Biopolymers.* 2015;104:213–246.
17. Chen L, Vasilatos SN, Qin Y, et al. *Oncotarget.* 2017;8:81737–81753.
18. Lim S, Janzer A, Becker A, et al. *Carcinogenesis.* 2010;31:512–520.
19. Hayami S, Kelly JD, Cho HS, et al. *Int J Cancer.* 2011;128:574–586.
20. Zheng YC, Ma J, Wang Z, et al. *Med Res Rev.* 2015;35:1032–1071.
21. Maes T, Mascaró C, Tirapu I, et al. *Cancer Cell.* 2018;33:495–511.
22. Fu X, Zhang P, Yu B. *Future Med Chem.* 2017;9:1227–1242.
23. Cloos PA, Christensen J, Agger K, et al. *Nature.* 2006;442:307–311.
24. Kruidenier L, Chung CW, Cheng Z, et al. *Nature.* 2012;488:404–408.
25. McAllister TE, England KS, Hopkinson RJ, Brennan PE, Kawamura A, Schofield CJ. *J Med Chem.* 2016;59:1308–1329.
26. Kang MK, Mehrazarin S, Park NH, Wang CY. *Oral Dis.* 2017;23:709–720.
27. Hatch SB, Yapp C, Montenegro RC, et al. *Epigenetics Chromatin.* 2017;10:9.
28. Plch J, Hrabeta J, Eckschlager T. *Int J Cancer.* 2019;144:221–231.
29. Taylor-Papadimitriou J, Burchell J. *Expert Opin Ther Targets.* 2017;21:5–7.
30. Pasini D, Hansen KH, Christensen J, Agger K, Cloos PA, Helin K. *Genes Dev.* 2008;22:1345–1355.
31. Teng YC, Lee CF, Li YS, et al. *Cancer Res.* 2013;73:4711–4721.
32. Hou J, Wu J, Dombkowski A, et al. *Am J Transl Res.* 2012;4:247–256.
33. Wang S, Wang Y, Wu H, Hu L. *PLoS ONE.* 2013;8:e84735.
34. Hayami S, Yoshimatsu M, Veerakumarasivam A, et al. *Mol Cancer.* 2010;9:59.
35. Stein J, Majores M, Rohde M, et al. *Am J Pathol.* 2014;184:2430–2437.
36. Kim TD, Shin S, Janknecht R. *Biochem Biophys Res Commun.* 2008;366:563–567.
37. Jangravi Z, Tabar MS, Mirzaei M, et al. *J Proteome Res.* 2015;14:3492–3502.
38. Westaway SM, Preston AGS, Barker MD, et al. *J Med Chem.* 2016;59:1370–1387.
39. Wu X, Fang Z, Yang B, et al. *Bioorg Med Chem Lett.* 2016;26:2284–2288.
40. Gehling VS, Bellon SF, Harmange JC, et al. *Bioorg Med Chem Lett.* 2016;26:4350–4354.
41. Liang J, Labadie S, Zhang B, et al. *Bioorg Med Chem Lett.* 2017;27:2974–2981.
42. Nie Z, Shi L, Lai C, et al. *Bioorg Med Chem Lett.* 2018;28:1490–1494.
43. Horton JR, Liu X, Wu L, et al. *J Med Chem.* 2018;61:3193–3208.
44. Itoh Y, Sawada H, Suzuki M, et al. *ACS Med Chem Lett.* 2015;6:665–670.
45. Vinogradova M, Gehling VS, Gustafson A, et al. *Nat Chem Biol.* 2016;12:531–538.
46. Johansson C, Velupillai S, Tumber A, et al. *Nat Chem Biol.* 2016;12:539–545.
47. Horton JR, Woodcock CB, Chen Q, et al. *J Med Chem.* 2018;61:10588–10601.
48. Suzuki T, Ozasa H, Itoh Y, et al. *J Med Chem.* 2013;56:7222–7231.
49. Hamada S, Suzuki T, Mino K, et al. *J Med Chem.* 2010;53:5629–5638.
50. Rose NR, Ng SS, Mecinovic J, et al. *J Med Chem.* 2008;51:7053–7056.
51. Đakovic M, Popovic Z. *Acta Cryst.* 2008;E64:m311–m312.
52. Abboud Y, Abourriche A, Saffaj T, et al. *Mater Chem Phys.* 2007;105:1–5.
53. Itoh Y, Nakashima Y, Tsukamoto S, et al. *Sci Rep.* 2019;9:767.